Published in "Plant Physiology doi:10.1104/pp.108.119420, 2008"
which should be cited to refer to this work.

Characterization and biological function of the *ISOCHORISMATE SYNTHASE 2* gene of *Arabidopsis thaliana*

Authors:

Christophe Garcion*, Antje Lohmann*, Elisabeth Lamodière, Jérémy Catinot, Antony Buchala, Peter Doermann, Jean-Pierre Métraux

Department of Biology, University of Fribourg, Route A. Gockel 3, 1700 Fribourg, Switzerland (E.L., J.C., A.B., J.P.M.); Institute of Molecular Physiology and Biotechnology of Plants (IMBIO), University of Bonn, Karlrobert-Kreiten-Strasse 13, 53115 Bonn, Germany (A.L., P.D.), UMR 1090 INRA-Université Bordeaux 2, 71 Avenue Edouard Bourlaux, 33140 Villenave d'Ornon (C.G.)

* These authors have contributed equally to this work.

Footnotes

This work was supported by the Swiss National Science Foundation (Grant # 3100A0–104224 to J.P. Métraux and by the German Science Foundation (Grant DFG Do520/8 to P. Doermann). Corresponding author: Jean-Pierre Métraux (e-mail: jean-pierre.metraux@unifr.ch).

The author responsible for distribution of materials integral to the findings presented in this article in accordance with the policy described in the Instructions for Authors (www.plantphysiol.org) is: Jean-Pierre Métraux (e-mail: jean-pierre.metraux@unifr.ch).

Abstract

Salicylic acid (SA) is an important mediator of plant defense response. In *Arabidopsis thaliana*, this compound was proposed to derive mainly from isochorismate, itself produced from chorismate through the activity of ICS1 (Isochorismate Synthase1). Null *ics1* mutants still accumulate some SA, suggesting the existence of an enzymatic activity redundant with ICS1 or of an alternative ICS-independent SA biosynthetic route. Here we studied the role of *ICS2*, second *ICS* gene of the Arabidopsis genome, in the production of SA. We have shown that *ICS2* encodes a functional ICS enzyme and that, similarly to ICS1, ICS2 is targeted to the plastids. Comparison of SA accumulation in the *ics1*, *ics2* and *ics1 ics2* mutants indicates that ICS2 participates in the synthesis of SA but in limited amounts, that become clearly detectable only when ICS1 is lacking. This unequal redundancy relationship was also observed for phylloquinone, another isochorismate-derived end-product. Furthermore, detection of SA in the double *ics1 ics2* double mutant that is completely devoid of phylloquinone provides genetic evidence of the existence of an ICS-independent SA biosynthetic pathway in Arabidopsis.

Introduction

SA has been linked in various species with diverse physiological aspects, like thermogenesis, stomatal closure, senescence, leaf abscision or resistance to abiotic stresses (Raskin, 1992; Morris et al., 2000, Martinez et al., 2004). SA is also a well-established regulatory component of the induced defense response in many plant species (Sticher et al., 1997). An increase in endogenous concentration of SA after an infection has been observed in many plants and correlated to the activation of defense mechanisms. The importance of the involvement of SA in the induction of resistance to oomycetes, bacterial or viral pathogens was demonstrated with mutants and transgenic plants that exhibit altered levels of SA (Sticher et al., 1997; Métraux and Durner, 2004; Garcion and Métraux, 2006). The pathway for SA biosynthesis and its regulation during infection has therefore become a central question in the understanding of induced plant resistance mechanisms. The biosynthesis of SA was first proposed to proceed through the benzoate pathway, as shown by studies based on radiolabeled compounds (Garcion and Métraux, 2006). In *A. thaliana*, a second pathway was proposed that is based on isochorismate, similar to the pathway described in some *Pseudomonas* species (Wildermuth et al., 2001). In this pathway, chorismate is converted into isochorismate through the action of an isochorismate synthase (ICS), and SA is generated from isochorismate by an isochorismate pyruvate-lyase. This scheme gained a strong support from studies with *ics1* mutants that accumulate only low levels of SA, although the conversion from isochorismate to SA has not yet been demonstrated in *Arabidopsis* (Wildermuth et al., 2001). The ICS1 gene product was confirmed to possess an ICS activity and to be targeted to the plastidic compartment (Strawn et al., 2007). Synthesis of SA following exposure to ozone in *Arabidopsis* was also suggested to proceed through the activity of ICS enzymes (Ogawa et al., 2005). The ICS pathway was recently shown to be active in tomato (Uppalapati et al., 2007) and *Nicotiana benthamiana* (Catinot et al., 2008). Furthermore, the isochorismate generated by the ICS is a precursor of phylloquinone, known as vitamin K1, which is a component of photosystem I (Gross et al., 2006). The involvement of isochorismate in the synthesis of this compound was further confirmed in

transgenic tobacco plants overexpressing an ICS of *Catharanthus roseus* and accumulating higher amounts of phylloquinone (Verberne et al., 2007). *C. roseus* or members of the *Rubiaceae* family also use isochorismate as a precursor for compounds such as anthraquinone or dihydroxybenzoates (Muljono et al., 2002; Mustafa and Verpoorte, 2005). However these molecules are taxon-specific and so far have not been investigated in *A. thaliana*.

The Arabidopsis genome contains a second *ICS* gene named *ICS2* (Wildermuth et al., 2001), but its biochemical activity relative to isochorismate production and its contribution to SA synthesis has not yet been clarified. In this article, we have addressed this question by isolating a full-length clone of *ICS2* and testing the activity and localization of its product relative to that of *ICS1*. We have also determined the amount of remaining SA in the *ics1*, *ics2* and *ics1ics2* mutants.

Results

Sequence Analysis of ICS1 and ICS2

Two isochorismate synthase genes, *ICS1* (At1g74710) and *ICS2* (At1g18870), are present in the genome of *A. thaliana*. These two genes belong to two blocks of approximately 3.5 Mb containing ordered fragments of similar sequence and therefore presumably originate from an ancient genomic duplication event (see http://wolfe.gen.tcd.ie/athal/dup)(Blanc et al., 2003). We first obtained a complete sequence of the *ICS2* in order to compare the nucleotide sequences of *ICS1* and *ICS2*. No full-length *ICS2* cDNA sequence was available from public databases and the current conceptual translation of the *ICS2* coding sequence, relying on ESTs, predicted an ICS2 protein sequence lacking a N-terminal extension compared to ICS1. We have isolated the 5' end of the *ICS2* messenger by using the rapid amplification of cDNA ends (RACE)-PCR technique, and then its full-length coding sequence by RT-PCR (accession EU589462). We found that the most 5'-located EST (N96097) matched our ICS2 cDNA sequence, but started at position 216 only, therefore did not include the first ATG start codon located at position 58 and suggested an erroneous start codon. The translation of the complete ICS2 coding sequence (562

amino acids) includes a N-terminal extension predicted to be a plastid-targeting peptide, unlike the current annotation for ICS2, but similarly to ICS1. Overall, ICS1 and ICS2 share 78 % of identity and 88 % of similarity at the amino acid level and are close to the characterized *Catharanthus roseus* CrICS (72 % of similarity with both ICS1 and ICS2; Fig. 1A) (van Tegelen et al., 1999). ICS1, ICS2 and CrICS contain the so-called chorismate-binding domain (Pfam accession PF00425), and conserved key residues consistent with an ICS catalytic activity (Kolappan et al., 2007).

At the genomic level, the *ICS2* gene contains 15 exons, compared to 13 for *ICS1*, but the overall exon/intron organization has been retained since the event that duplicated the *ICS* genes (Fig. 1B). Minor exceptions are the splitting of exons 3 and 4 of *ICS1* into exons 3 to 6 of *ICS2*, or alternatively the fusion of exons 3-6 of *ICS2* into the exons 3 and 4 of *ICS1*.

Subcellular Localization of ICS1 and ICS2

Analysis of the ICS1 and ICS2 sequences with the TargetP (Emanuelsson et al., 2000) and Predotar (Small et al., 2004) softwares suggested that both proteins contained a plastid targeting signal. The predicted localization in plastids is consistent with the production of the chorismate substrate in these organelles. Plastid localization of ICS1 and ICS2 was tested by fusing their coding sequence to GFP and transiently expressing these constructs in tobacco cells. Observations of the transformed cells with a laser confocal microscope clearly showed that the GFP fluorescence colocalized with chlorophyll fluorescence, indicating that both fusion proteins were located within the chloroplasts (Fig. 2). As a control, we expressed GFP alone following the same protocol and observed a cytosolic signal.

Characterization of ICS1 and ICS2 Enzymatic Activity

ICS1 was initially proposed to catalyze the conversion of chorismate into isochorismate based on sequence similarity with a characterized ICS from *Catharanthus roseus* (Wildermuth et al., 2001). To determine experimentally whether ICS1 but also ICS2 truly possess such an ICS enzymatic activity, we relied on a functional complementation assay. In *E. coli*, an endogenous ICS activity is required for production of enterobactin, a high-

affinity iron ligand secreted in the medium and internalized following iron chelation (Raymond et al., 2003). Iron scavenging by microorganims can be monitored easily using the CAS (chrome azurol sulfonate) medium devised by Schywn and Neilands (1987). This medium contains a dye that forms an intense blue complex with iron, and turns orange when iron has been transferred to another iron-binding molecule. For our functional assay we used PBB8, a mutant of *E. coli* that lacks endogenous ICS activity and is therefore unable to produce enterobactin (Muller et al., 1996) (Fig. 3). As a positive control, we have used the *E. coli EntC* gene encoding an ICS, that restored enterobactin production after introduction into the PBB8 strain, and entailed the formation of an orange halo around positive colonies (Fig. 3). PBB8 cells expressing *ICS1* under the control of the strong IPTG-inducible Ptac promoter also showed an orange halo even without induction by IPTG, indicating that *ICS1* could complement the PBB8 *ICS* deficiency. No significant coloration was observed for cells expressing *ICS2* under the same conditions. However, induction by IPTG at 0.2 mM lead to the appearance of the orange signature for siderophore production (Fig. 3) thus demonstrating that *ICS2* encodes functional ICS enzymes similarly to *ICS1*.

The apparent difference of response to IPTG between *ICS1* and *ICS2* in the CAS assay was not due to variations of the expression system since both were cloned in the same vector, under the control of the same promoter and 5'UTR, after removal of the transit peptide-coding sequence. Expression problems due to codon bias were also prevented by using the pRARE plasmid throughout the experiment (Novy et al., 2001). Instead, we observed that the ICS2 protein accumulated at much lower levels than ICS1 in *E. coli* cells by using tagged versions of ICS1 and ICS2 (data not shown).

Expression of ICS1 and ICS2 in *E. coli* also allowed to test whether these two enzymes could generate SA directly from chorismate. No SA accumulated in cell cultures, unlike cells expressing the positive control PchB from *Pseudomonas aeruginosa* (Gaille et al., 2002), therefore suggesting that ICS1 and ICS2 have no isochorismate pyruvate lyase (IPL) activity (data not shown).

Phylloquinone Accumulation in *ics* Mutants

In order to determine the relative contribution of ICS1 and ICS2 to isochorismate production, we used the following mutants: *ics1* (*sid2-1* allele (Nawrath and Métraux, 1999)) and *ics2* (carrying a T-DNA insertion in the *ICS2* gene of *Arabidopsis* (SALK_084635)). Neither of these single mutants exhibited a striking visual phenotype compared to the wild type (Fig. 4A). We focused our study on phylloquinone and SA, presumably both derived from isochorismate in *A. thaliana*. Phylloquinone was measured in the *ics1* and *ics2* mutant lines by fluorescence HPLC after reduction of phylloquinone to the phyllohydroquinone form according to Lohmann et al (2006). The pylloquinone content in leaves of *ics1* was reduced to ca. 35 % of WT indicating that the *ICS1* gene product provides the predominant amount of isochorismate required for phylloquinone synthesis (Fig. 4B). The amount of phylloquinone of the homozygous *ics2* mutant was not different from WT (Fig. 4B). Although the phylloquinone content in *ics1* was strongly reduced, the total chlorophyll content was not affected (1169 ± 62, 1182 ± 61 and 1208 ± 103 µg.g FW-1 in WT, *ics1* and *ics2*, respectively).

The functional overlap between ICS1 and ICS2 was investigated in double homozygous *ics1ics2* mutants. F2 plants derived from a cross of *ics1* and *ics2* were raised on sucrose containing medium and screened for double homozygous lines by phylloquinone measurements and by PCR using oligonucleotides designed for the *ics2* locus. Double homozygous *ics1ics2* mutants remained smaller than the WT and single mutants, and displayed a pale green to yellowish pigmentation (Fig. 4A). Beside this strong reduction in growth, they could only be maintained on sucrose medium. The novel growth defects present in the double mutant compared to the single mutants indicated that both genes were dispensable but not together, and that at least one was required and sufficient for normal growth under these conditions. This defines a symmetrical, or equal redundancy between ICS1 and ICS2 in respect to the ability to grow under standard conditions. Double homozygous mutant lines (*ics1 ics2*) were totally devoid of phylloquinone (Fig. 4B). Plants homozygous for the *ics1* mutation, but heterozygous for *ics2* contained significantly less phylloquinone (19 % of WT, data not shown) than *ics1* single mutants (35 % of WT, see above)(also see Gross et al., 2006), suggesting that the ICS2 enzyme becomes limiting for isochorismate production in the *ics1* mutant background.

SA Accumulation in *ics* Mutants

SA is presumed to derive from isochorismate in *Arabidopsis*, since SA accumulation was shown to be severely impaired in the *ics1* mutant upon inducing conditions (Nawrath and Métraux, 1999; Wildermuth et al., 2001). We have analyzed the induction of SA accumulation in the *ics1*, *ics2* and *ics1 ics2* mutants after UV-treatment, a known stimulus for SA accumulation (Nawrath et al., 2002). As expected, the *ics1* mutant accumulated roughly 10% of total SA compared to the wild type (0.47±0.14 versus 4.17±1.26 µg.g FW^{-1} respectively) (Fig. 4C). The mean value for the *ics2* mutant was similar to the wild-type reference (4.13±1.27 versus 4.17±1.26 µg.g FW^{-1}) (Fig. 4C). Therefore in the WT the *ics2* mutation does not have a high impact on SA accumulation upon UV exposure or in a non-induced state (0.54±0.09 versus 0.56±0.12 µg.g FW^{-1}). This result was expected following the simple reasoning that if (i) ICS1 and ICS2 were independently regulated, and if (ii) ICS1 accounted for approximately 90% of the total amount of isochorismate produced in these conditions (phenotype of the *ics1* mutant), then ICS2 at best would contribute to only 10% of isochorismate production in these conditions, and consequently an *ics2* mutant should not be strongly affected in SA accumulation.

We then determined if ICS2 was required for the production of the remaining SA in the *ics1* mutant, and evaluated the genetic relationship between *ICS1* and *ICS2* in the course of SA biosynthesis after UV-induction using the *ics1ics2* double mutant. Without any induction, *ics1 ics2* double mutants accumulated approximately 43% of total SA relative to the *ics1* mutant (0.12±0.08 versus 0.28±0.09 µg.g FW^{-1})(Fig. 4c). The difference in SA accumulation between the *ics1* and *ics1 ics2* mutants can be assigned to the activity of the *ICS2* gene product. The same effect was observed after UV stimulation, since the *ics1 ics2* double mutant produced total SA in a similar range of about 36% relative to the *ics1* mutant (0.17±0.12 versus 0.47±0.14 µg.g FW^{-1})(Fig. 4c). The structure of SA in the double mutant was verified by GC-MS (Fig. 5). These results imply that ICS2 can be involved in the SA biosynthesis through isochorismate production, however its contribution is marginal compared to ICS1. Since the values before and after UV-

induction are not statistically very different both for the *ics1* and *ics1 ics2* mutants, we can further conclude that unlike *ICS1, ICS2* does not display a strong inducible activity following UV irradiation. The detection of SA in the double *ics1 ics2* mutant, that is devoid of plastid ICS activity as suggested from the absence of phylloquinone, indicates that an alternative SA biosynthetic pathway is active. Our data show that this pathway is not inducible by UV irradiation and accounts for minor amounts of total SA production (about 20% in uninduced state and 4% after UV induction).

Discussion

SA plays a major role in a number of physiological responses and defense reactions, yet some aspects of its biosynthesis still remain unknown. In particular, this concerns the implication of the two *Arabidopsis ICS* genes in the biosynthesis of SA. In this work we have characterized the *A. thaliana* ICS1 and ICS2 gene products and evaluated their respective contribution to isochorismate-derived compounds in this species, namely SA and phylloquinone.

The existence of two ICS genes in *Arabidopsis* raises the issue of their specificity and the extent of their redundancy. However, not all higher plants have two distinct *ICS* genes. In rice (*Oryza sativa japonica*) there is only one *ICS* gene and this gene has not been studied so far. In this species, SA derives from a phenylalanine ammonia lyase (PAL)-dependent pathway (Silverman et al., 1995; Sawada et al., 2006). However the regulation of SA synthesis and metabolism in rice might be different from other plant species since SA is present in very high levels as a free acid, and might serve alternative functions (Yang et al., 2004). In poplar, a single *ICS* gene has been detected (Tsai et al., 2006). For this species the involvement of ICS in the synthesis of its numerous potential SA glycoside and of phylloquinone has not yet been explored. So far, no generalization can be drawn from these model organisms since each of them is known to have a specific metabolism for SA. The recent draft sequence of the grapevine genome also suggests that there is only one *ICS* gene in this species, although three ancestral genomes have been detected (Jaillon et al., 2007). The uniqueness of the *ICS* gene in poplar, rice and grapevine may

constitute a state of evolution where other duplicated *ICS* genes have been lost, and a single gene takes over the production of the common precursor of phylloquinone and SA. The existence of two *ICS* genes in the *Arabidopsis* genome may thus appear as an exception arising from our consideration of this genome at this time instead of in the course of its evolution. The two *ICS* genes occur within duplicated blocks that originate from a large genomic duplication (Blanc et al., 2003). On the one hand, the less obvious role of *ICS2* compared to *ICS1* might indicate that *ICS2* could be lost in the future without loss of fitness. On the other hand, this gene could also provide a benefit for the plant in the field or yet undiscovered conditions, which would justify why ICS2 has not been already lost. It is interesting to note that in *Catharantus roseus* only one gene, but two different ICS isoforms have been detected after elicitation of cell cultures (van Tegelen et al., 1999). It is possible that in this species the supplementary function of isochorismate as a precursor of 2,3-dihydroxybenzoic acid is associated with a specific regulation of the ICS gene product.

It is not known whether only one of the two Arabidopsis ICS would contribute to a specific biological process. The data from the *ics* mutants (Fig. 4) indicate that both participate in the synthesis of SA and phylloquinone. This is consistent with the observation that both are targeted to the same subcellular compartment. Moreover, a recent study has suggested that the gene products involved in the phylloquinone biosynthesis may form enzymatic complexes in the stroma (Kim et al., 2008). However the ubiquitous stromal localization of both of the ICS:GFP fusions (Fig. 3) indicates that neither ICS1 nor ICS2 is presumably restricted to these complexes. This localization suggests that the isochorismate produced by both of the enzymes then diffuses up to the subsequent active centers that catalyze phylloquinone formation.

A tight regulation of duplicated genes is observed in prokaryotes and correlates with their genomic organization in operons. In *Escherichia coli*, two *ICS* genes have been described and each of them is linked to a distinct pathway. The *EntC* gene is part of an operon associated with the synthesis of enterobactin, a dihydroxybenzoate-derived siderophore, and is regulated following iron requirement (Kwon et al., 1996). The MenF gene is

involved in the synthesis of menaquinone (also known as vitamin K2), an electron-carrier in the respiratory chain during anaerobic growth (Jiang et al., 2007). MenF is induced only during anoxygenic conditions. Due to this tight regulation, the two ICS genes show a low redundancy (Dahm et al., 1998; Buss et al., 2001). A somewhat different situation has been described for *Bacillus subtilis*, where one of the two ICS can provide isochorismate for dihydroxybenzoate and menaquinone production, but the other one is active only in menaquinone synthesis (Rowland and Taber, 1996). In *Arabidopsis*, our study established that although ICS1 and ICS2 are involved in both SA and phylloquinone production, the absence of ICS2 produced a less dramatic effect than the absence of ICS1 on SA and phylloquinone accumulation. That is, the activity of ICS1 could largely compensate for the absence of ICS2, but the ICS2 activity could not make up for a genetic lesion in *ICS1*. Therefore *ICS1* and *ICS2* constitute an example of unequal redundancy as defined by (Briggs et al., 2006).

Transcriptional regulation might provide part of a mechanistic interpretation of these results. Microarray data available through Genevestigator (Zimmermann et al., 2005) indicate that both *ICS1* and *ICS2* are expressed at low levels in non-inducing conditions. The resulting low-level constitutive ICS activity correlates with the continuous requirement of phylloquinone from the plant, in order to sustain a continuous growth and development. Phylloquinone is an essential component of photosystem I where it functions as an electron acceptor (Gross et al., 2006). Visual inspection of the single *ics1* and *ics2* mutant would suggest that ICS1 and ICS2 are equally redundant, however phylloquinone measurement revealed that ICS1 played a greater role in phylloquinone accumulation than ICS2. A threshold effect for phylloquinone requirement for growth and development is likely responsible for this discrepancy. The different requirements for the respective ICS gene products suggests that in these non-inducing conditions ICS1 is more accumulated or active than ICS2, maybe because of differences in the transcript accumulation rate, translation efficiency, other post-translational control or catalytic activity or regulation. A less straightforward possibility to interpret the phenotype of phylloquinone accumulation of the single mutants would be that the absence of one ICS gene product is compensated by increased activity of the other remaining functional *ICS*

gene; differences in the efficiency of this negative feed-back control loop for regulation of *ICS1* or *ICS2* would also lead to apparent unequal importance of the two genes.

Specific induction of ICS1 mRNA accumulation, but not of ICS2 mRNA, under some SA-inducing conditions such as biotic (Wildermuth et al., 2001) or abiotic stresses, e.g. UV-C, ozone (data not shown) (Zimmermann et al., 2005) provides an obvious explanation to the stronger requirement for ICS1 rather than ICS2 for SA biosynthesis, and therefore explains the phenotype of the mutants relative to their SA accumulation. Alternatively, post-transcriptional mechanisms or enzymatic properties could also be postulated to explain the major role of ICS1 compared to ICS2. Interestingly, specific stimuli can also induce the *ICS2* gene, either in conjunction with *ICS1* (i.e. senescence), or without induction of *ICS1* (i.e. ABA treatment; data not shown) (Zimmermann et al., 2005), suggesting that ICS2 could play a role yet to be discovered. Careful inspection of the *ics2* mutant subjected to such stimuli did not reveal obvious phenotypical changes (data not shown). So far these data suggest that a major difference between *ICS1* and *ICS2* rely on transcriptional regulation.

SA biosynthesis in *A. thaliana* has been proposed to proceed for a large extent through the catalytic activity of the ICS genes (Wildermuth et al., 2001). However the *ics1* mutant still exhibit 5-10% of SA compared to the WT after an adequate stimulation. The presence of SA in this mutant indicates either a redundant ICS activity or an alternative biosynthetic pathway such as the phenylpropanoid pathway as proposed by previous studies in *A. thaliana* (Mauch-Mani and Slusarenko, 1996; Ferrari et al., 2003). Here we have assessed the contribution of ICS2 in the production of SA in the *ics1* mutant using a genetic approach. Our data indicate a low but detectable residual level of SA in the double mutant *ics1 ics2* supporting the existence of an ICS-independent biosynthetic pathway for SA. The susceptibility of the *ics1* mutant suggests that SA produced through ICS1 is biologically active and important for defense reactions (Wildermuth et al., 2001). Other studies in *A. thaliana* have proposed that biologically active SA is mainly made from a pathway derived from phenylpropanoids. However, these results might be questioned for the following reasons. In the first study, SA levels were determined using HPLC separation and detected by absorption at 280 nm (Mauch-Mani and Slusarenko,

1996). At this wavelength SA is hardly detectable for the amounts present in leaf extracts of *A. thaliana* and fluorescence detection is required for a reasonable readout. This leaves some uncertainty over the nature of the metabolite measured as SA in this report. In another study, the production of biologically relevant SA from an ICS-independent pathway was mainly inferred from biological effects on resistance against *Botrytis cinerea* using treatments with 2-aminoindane 2-phosphonic acid, an inhibitor of PAL (Ferrari et al., 2003). The effect of these treatments on SA accumulation in the tissue was however not determined.

In conclusion, we have demonstrated the function and localization of ICS2 involved in SA biosynthesis. Using *ics1*, *ics2* and *ics1 ics2* mutants we have demonstrated that ICS2 contributes to SA but in limited amounts, detectable only when ICS1 is lacking. This unequal redundancy was also observed for phylloquinone production. Furthermore, detection of SA in *ics1 ics2* that is completely devoid of phylloquinone provided genetic evidence of the existence of an ICS-independent SA biosynthetic pathway in *A. thaliana*.

Material and Methods

Plant material and growth conditions

Plants were grown on a pasteurized soil mix of humus/perlite (3:1) under a 12-h-light and 12-h-dark cycle, with a night temperature of 16°C and a day temperature of 20-22°C. Arabidopsis accession Col-0 was obtained from the Arabidopsis Biological Research Center (Columbus, OH). The T-DNA insertion mutant *ics2* (SALK_084635) (Alonso et al., 2003) was obtained from the Nottingham Arabidopsis Seed Center.

RACE-PCR reactions

We used the First-Choice RLM RACE kit (Ambion, Rotkreuz, Switzerland) to determine the 5'end of the ICS2 messenger, following instructions recommended by the manufacturer.

Subcellular localization

GFP fusions were realized by using the Gateway technology. ICS1 and ICS2 cDNAs were amplified from reverse-transcription products with Pfu polymerase (Stratagene, Amsterdam, Netherlands) using primers ICS1-6 (CACCATGGCTTCACTTCAATTTTCT) and ICS1-8 (ATTAATCGCCTGTAGAGATG), and ICS2-5 (CACCATGGCGTCGCTTCAGTGTTCA) and ICS2-7 (GTTGATTGGTTGCAAAGCTGA) respectively, then cloned into the entry vector pENTR-D-Topo (Invitrogen, Basel Switzerland). Entry clones were then recombined with the pB7FWG2 vector (Karimi et al., 2005), generating cDNA-GFP fusions driven by the CaMV35S promoter. The pB7F2 control vector was generated by digestion of pB7FWG2 with EcoRV followed by self-ligation, thus removing the *ccdB* cassette and placing GFP directly under the control of the CaMV 35S promoter. The vectors were then transformed into *Agrobacterium tumefaciens* strain GV3101. The *Agrobacterium* infiltration procedure was realized as described (Burch-Smith et al., 2006) except that the 50-ml culture step was omitted and that acetosyringone was used at 100 µM. Infiltrated patches of leaves were observed after 3 to 4 days with a Bio-Rad MRC 1024 laser confocal microscope. For imaging GFP and chlorophyll, excitation was at 488 nm and 647 nm respectively, and emissions were collected with a 506-538 nm band-pass filter (referred as 522DF32) and a 664-696 nm band-pass filter (referred as 680DF32) respectively.

Functional complementation of the PBB8 strain of E. coli

Empty vector pJF119EH1 and EntC-overexpressing construct pDF2 (Franke et al., 2003) were a kind gift from G. Sprenger (Stuttgart, Germany). ICS1 coding sequence without the first 45 amino acids was flanked with NcoI and BamHI restriction sites by amplification with primers ICS1-1 (AACTTTAAGAAGGAGATATACCATGGCATATGCTATGTCTATGAATGGTTGT GAT) and ICS1-2 (GGATCCTCAATTAATCGCCTGTAGAGA) and was sub-cloned into the pGEM-T-Easy vector (Promega). An EcoRI-BamHI fragment from this contruct was then inserted into pJF119EH1 to give pJF202. The ICS2 coding sequence without the first 50 amino acids was amplified with primers ICS2-8

(CTTTAAGAAGGAGATATACCATGGCAAACGGATGTGAGGCTGACCAC) and ICS2-9 (GGATCCTTAGTTGATTGGTTGCAAAGC) and then subcloned into pJF202 as a NcoI-BamHI fragment, giving pJF608. These constructs were introduced into the *entC*$^{-}$ *MenF*$^{-}$ PBB8 *E. coli* strain (Muller et al., 1996), previously tranformed with the pRARE plasmid (Novy et al., 2001). The PBB8 strain was kindly provided by E. Leistner (Bonn, Germany). Individual colonies were allowed to grow for 6h in 400 µl of LB medium containing ampicillin and chloramphenicol; bacterial cells were then rinsed in MgSO4 (10mM) and plated onto CAS agar (Schwyn and Neilands, 1987) supplemented with 10% casaminoacids (BD Biosciences, Allschwil, Switzerland).

Determination of the genotype of the *ICS2 locus*

The primers ICS2-1 (GTCTTCAAAGTCTCCTCTGAT) and ICS2-2 (TGAATCACCTCTAGGCCTTGT) were used to detect a wild-type copy of the *ICS2* gene by PCR. The T-DNA disrupted allele (Alonso et al., 2003) was detected by using primers ICS2-2 and Lba1 (TGGTTCACGTAGTGGGCCATCG). PCR reactions for investigating the presence of WT and mutant alleles were run separately.

Phylloquinone determination

Phylloquinone was measured in the *ics1* and *ics2* mutants by fluorescence HPLC after reduction of phylloquinone to the phyllohydroquinone form (Lohmann et al., 2006).

SA extraction and quantification by HPLC

Samples were taken from leaves of plants grown on MS medium supplemented with 1% sucrose 18 h after exposure to UV-C light for stimulation of SA accumulation (Nawrath and Métraux, 1999). SA was extracted and total SA (free and conjugated) quantified using a modification of the method previously described (Nawrath and Métraux, 1999). Leaf tissue (0.2 to 0.3 g with 1.5 µg *o*-anisic acid as internal standard) was extracted twice with 2 ml of 100 % methanol each. After evaporation of methanol from the combined extracts, acid hydrolysis was performed with 4 N HCl at 80 °C for 1 hr, and SA was extracted twice with 2 ml ethyl acetate/hexane (1:1). The combined organic extracts were evaporated, re-dissolved in 50 µl acetonitrile of which 20 µl were injected

on a reverse phase HPLC column (ABZ+, 250 mm x 4.6 mm; Supelco, Munich, Germany) and separated at a flow rate of 1 ml min^{-1} (Agilent 1100 HPLC System, Böblingen, Germany). Elution began with an isocratic flow of 15 % acetonitrile in water (pH 2.6 adjusted with phosphoric acid) for 1 min, followed by a linear increase to 20 % acetonitrile over 5 min, isocratic elution at 20 % for 10 min, a linear increase from 20 to 55 % acetonitrile over 9.5 min, and to 90 % in 5 min. For column regeneration, acetonitrile was decreased linearly from 90 % to 0 %, followed by a linear increase to 15 % acetonitrile and an isocratic flow at 15 % for 4 min. Fluorescence was recorded with excitation/emission/ wavelengths of 305/365 nm and 305/407 nm for o-anisic acid and SA, respectively (Dewdney et al., 2000).

GC–MS analysis of SA

For GC-MS analysis, the SA samples were extracted as described above. After evaporation of solvent, 50 µl of MSTFA (N-Methyl-N-trimethylsilyl-trifluoracetamide) was added, and the samples were incubated for 1 hr at 80 °C for silylation. After the evaporation of MSTFA, the extracts were re-dissolved in 40 µl hexane. The trimethylsilyl (TMS) derivatives of SA were analyzed by GC using an Agilent 6890 system (Agilent, Böblingen, Germany) equipped with an Agilent 5973 quadrupole mass detector. The inlet was maintained at 260 °C and operated in the splitless mode (injection volume 1 µl). A 30 m × 530 µm and 0.2 µm film thickness SP-2380 column (Supelco, Munich, Germany) was used for analyses with a Helium flow of 5.1 ml min^{-1}. The initial oven temperature was 80°C and was then ramped to 180°C at a rate of 1°C min^{-1}. The oven temperature was maintained at 180°C for 1 min and decreased to 80°C with a rate of 20°C min^{-1}. Silylated SA and o-anisic acid were detected at m/z 267 and 209, respectively.

Acknowledgements

We would like to acknowledge Linda Grainger for technical assistance, Martine Schorderet for confocal microscope assistance, and Eliane Abou-Mansour for help with SA analysis. We thank Pr. G. Sprenger (Stuttgart, Germany) for sharing plasmids

PJF119EH1 and pDF2, and Pr. E. Leistner (Bonn, Germany) for providing the PBB8 *E. coli* strain.

Literature cited

Alonso JM, Stepanova AN, Leisse TJ, Kim CJ, Chen HM, Shinn P, Stevenson DK, Zimmerman J, Barajas P, Cheuk R, et al (2003) Genome-wide insertional mutagenesis of *Arabidopsis thaliana*. Science **301:** 653-657

Blanc G, Hokamp K, Wolfe KH (2003) A recent polyploidy superimposed on older large-scale duplications in the *Arabidopsis genome*. Genome Res **13:** 137-144

Briggs GC, Osmont KS, Shindo C, Sibout R, Hardtke CS (2006) Unequal genetic redundancies in Arabidopsis - a neglected phenomenon? Trends Plant Sci **11:** 492-498

Burch-Smith TM, Schiff M, Liu YL, Dinesh-Kumar SP (2006) Efficient virus-induced gene silencing in Arabidopsis. Plant Physiol **142:** 21-27

Buss K, Muller R, Dahm C, Gaitatzis N, Skrzypczak-Pietraszek E, Lohmann S, Gassen M, Leistner E (2001) Clustering of isochorismate synthase genes menF and entC and channeling of isochorismate in *Escherichia coli*. Biochim & Biophys Acta-Gene Struct Expr **1522:** 151-157

Catinot J, Buchala A, Abou-Mansour E, Métraux JP (2008) Salicylic acid production in response to biotic and abiotic stress depends on isochorismate in *Nicotiana benthamiana*. FEBS Letters **582:** 473-478

Dahm C, Muller R, Schulte G, Schmidt K, Leistner E (1998) The role of isochorismate hydroxymutase genes entC and menF in enterobactin and menaquinone biosynthesis in *Escherichia coli*. Biochim & Biophys Acta-Gen Subjects **1425:** 377-386

Dewdney J, Reuber TL, Wildermuth MC, Devoto A, Cui JP, Stutius LM, Drummond EP, Ausubel FM (2000) Three unique mutants of Arabidopsis identify *eds* loci required for limiting growth of a biotrophic fungal pathogen. Plant J **24:** 205-218

Emanuelsson O, Nielsen H, Brunak S, von Heijne G (2000) Predicting subcellular localization of proteins based on their N-terminal amino acid sequence. J Mol Biol **300:** 1005-1016

Ferrari S, Plotnikova JM, De Lorenzo G, Ausubel FM (2003) Arabidopsis local resistance to *Botrytis cinerea* involves salicylic acid and camalexin and requires EDS4 and PAD2, but not SID2, EDS5 or PAD4. Plant J **35: 193-205**

Franke D, Lorbach V, Esser S, Dose C, Sprenger GA, Halfar M, Thommes J, Muller R, Takors R, Muller M (2003) (S,S)-2,3-Dihydroxy-2,3-dihydrobenzoic acid: microbial access with engineered cells of *Escherichia coli* and application as starting material in natural-product synthesis. Chemistry **9:** 4188-4196

Gaille C, Kast P, Haas D (2002) Salicylate biosynthesis in *Pseudomonas aeruginosa*. Purification and characterization of PchB, a novel bifunctional enzyme displaying isochorismate pyruvate-lyase and chorismate mutase activities. J Biol Chem **277:** 21768-21775

Garcion C, Métraux JP (2006) Salicylic acid. *In* P Hedden, SG Thomas, eds, Plant hormone signaling. Annu Plant Rev Vol. 24. Blackwell Press, Oxford, pp 229-257

Gross J, Cho WK, Lezhneva L, Falk J, Krupinska K, Shinozaki K, Seki M, Herrmann RG, Meurer J (2006) A plant locus essential for phylloquinone (vitamin K1) biosynthesis originated from a fusion of four eubacterial genes. J. Biol Chem **281:** 17189-17196

Jaillon O, Aury JM, Noel B, Policriti A, Clepet C, Casagrande A, Choisne N, Aubourg S, Vitulo N, Jubin C, et al (2007) The grapevine genome sequence suggests ancestral hexaploidization in major angiosperm phyla. Nature **449:** 463-465

Jiang M, Cao Y, Guo ZF, Chen MJ, Chen XL, Guo ZH (2007) Menaquinone biosynthesis in *Escherichia coli*: Identification of 2-succinyl-5-enolpyruvyl-6-

hydroxy-3-cyclohexene-l-carboxylate as a novel intermediate and re-evaluation of MenD activity. Biochem **46:** 10979-10989

Karimi M, De Meyer B, Hilson P (2005) Modular cloning in plant cells. Trends Plant Sci **10:** 103-105

Kim HU, van Oostende C, Basset GJC, Browse J (2008) The *AAE14* gene encodes the Arabidopsis o-succinylbenzoyl-CoA ligase that is essential for phylloquinone synthesis and photosystem-I function. Plant J. in press

Kolappan S, Zwahlen J, Zhou R, Truglio JJ, Tonge PJ, Kisker C (2007) Lysine 190 is the catalytic base in MenF, the menaquinone-specific isochorismate synthase from *Escherichia coli*: Implications for an enzyme family. Biochem **46:** 946-953

Kwon O, Hudspeth MES, Meganathan R (1996) Anaerobic biosynthesis of enterobactin in *Escherichia coli*: Regulation of *entC* gene expression and evidence against its involvement in menaquinone (vitamin K-2) biosynthesis. J Bacteriol **178:** 3252-3259

Lohmann A, Schottler MA, Brehelin C, Kessler F, Bock R, Cahoon EB, Dormann P (2006) Deficiency in phylloquinone (vitamin K1) methylation affects prenyl quinone distribution, photosystem 1 abundance, and anthocyanin accumulation in the Arabidopsis *atmeng* mutant. J Biol Chem **281:** 40461-40472

Martinez C, Pons E, Prats G, Leon J (2004) Salicylic acid regulates flowering time and links defence responses and reproductive development. Plant J. **37**(2):209-17.

Mauch-Mani B, Slusarenko AJ (1996) Production of salicylic acid precursors is a major function of phenylalanine ammonia-lyase in the resistance of Arabidopsis to *Peronospora parasitica*. Plant Cell **8:** 203-212

Métraux JP, Durner J (2004) The role of salicylic acid and nitric oxide in programmed cell death and induced resistance. *In* H Sandermann, ed, Ecological Studies, Vol 170. Springer-Verlag, Berlin, Heidelberg, pp 111-150

Morris K, Mackerness SAH, Page T, John CF, Murphy AM, Carr JP, Buchanan-Wollaston V (2000) Salicylic acid has a role in regulating gene expression during leaf senescence. Plant J **23:** 677-685

Muljono RAB, Scheffer JC, Verpoorte R (2002) Isochorismate is an intermediate in 2,3-dihydroxybenzoic acid biosynthesis in *Catharanthus roseus* cell cultures. Plant Physiol Biochem **40:** 231-234

Muller R, Dahm C, Schulte G, Leistner E (1996) An isochorismate hydroxymutase isogene in *Escherichia coli*. FEBS Letters **378:** 131-134

Mustafa NR, Verpoorte R (2005) Chorismate derived C6C1 compounds in plants. Planta **222:** 1-5

Nawrath C, Heck S, Parinthawong N, Métraux JP. (2002) EDS5, an essential component of salicylic acid-dependent signaling for disease resistance in Arabidopsis, is a member of the MATE transporter family. *Plant Cell* **14:** 275-286

Novy R, Drott D, Yaeger K, Mierendorf R (2001) Overcoming the codon bias of *E. coli* for enhanced protein expression. InNovations **12:** 1-3

Ogawa D, Nakajima N, Sano T, Tamaoki M, Aono M, Kubo A, Kanna M, Ioki M, Kamada H, Saji H (2005) Salicylic acid accumulation under O-3 exposure is regulated by ethylene in tobacco plants. Plant Cell Physiol **46**: 1062-1072

Raskin I (1992) Salicylate, a new plant hormone. Plant Physiol **99:** 799-803

Raymond KN, Dertz EA, Kim SS (2003) Enterobactin: an archetype for microbial iron transport. Proc Natl Acad Sci USA **100:** 3584-3588

Rowland BM, Taber HW (1996) Duplicate isochorismate synthase genes of *Bacillus subtilis*: Regulation and involvement in the biosyntheses of menaquinone and 2,3-dihydroxybenzoate. J Bacteriol **178**: 854-861

Sawada H, Shim IS, Usui K (2006) Induction of benzoic acid 2-hydroxylase and salicylic acid biosynthesis - Modulation by salt stress in rice seedlings. Plant Sci **171:** 263-270

Schwyn B, Neilands JB (1987) Universal chemical-assay for the detection and determination of siderophores. Anal Biochem **160:** 47-56

Silverman P, Seskar M, Kanter D, Schweizer P, Métraux JP, Raskin I (1995) Salicylic-acid in rice - biosynthesis, conjugation, and possible role. Plant Physiol **108:** 633-639

Small I, Peeters N, Legeai F, Lurin C (2004) Predotar: A tool for rapidly screening proteomes for N-terminal targeting sequences. Proteomics **4:** 1581-1590

Sticher L, Mauch-Mani B, Métraux JP (1997) Systemic acquired resistance. Ann Rev Phytopathol **35: 235-270**

Strawn MA, Marr SK, Inoue K, Inada N, Zubieta C, Wildermuth MC (2007) Arabidopsis isochorismate synthase functional in pathogen-induced salicylate biosynthesis exhibits properties consistent with a role in diverse stress responses. J Biol Chem **282:** 5919-5933

Tsai CJ, Harding SA, Tschaplinski TJ, Lindroth RL, Yuan YN (2006) Genome-wide analysis of the structural genes regulating defense phenylpropanoid metabolism in *Populus*. New Phytol **172**: 47-62

Uppalapati SR, Ishiga Y, Wangdi T, Kunkel BN, Anand A, Mysore KS, Bender CL (2007) The phytotoxin coronatine contributes to pathogen fitness and is required for suppression of salicylic acid accumulation in tomato inoculated with *Pseudomonas syringae* pv. *tomato* DC3000. Mol Plant Microbe Interact **20:** 955-965

van Tegelen LJP, Moreno PRH, Croes AF, Verpoorte R, Wullems GJ (1999) Purification and cDNA cloning of isochorismate synthase from elicited cell cultures of *Catharanthus roseus*. Plant Physiol **119:** 705-712

Verberne MC, Sansuk K, Bol JF, Linthorst HJM, Verpoorte R (2007) Vitamin K-1 accumulation in tobacco plants overexpressing bacterial genes involved in the biosynthesis of salicylic acid. J Biotech **128:** 72-79

Wildermuth MC, Dewdney J, Wu G, Ausubel FM (2001) Isochorismate synthase is required to synthesize salicylic acid for plant defence. Nature **417:** 562-565

Yang YN, Qi M, Mei CS (2004) Endogenous salicylic acid protects rice plants from oxidative damage caused by aging as well as biotic and abiotic stress. Plant J **40:** 909-919

Zimmermann P, Hennig L, Gruissem W (2005) Gene-expression analysis and network discovery using Genevestigator. Trends Plant Sci **10:** 407-409

Legends of figures

Figure 1.

A. Sequence alignement of *Arabidopsis thaliana* ICS1(NP_565090) and ICS2 (ACC60228) and *Catharanthus roseus* ICS (CAA06837). The chorismate-binding domain is located in the dashed area and the position of residues conserved in ICS enzymes (Kolappan et al., 2007) is indicated with a star.

B. Exon/intron structure of ICS1 and ICS2. Exons are represented by grey boxes and introns by thin lines. Sequence similarity between exon 3 of AtICS1 and 3 and 4 of ICS2, and 4 of AtICS1 and 5 and 6 of ICS2 is highlighted by dashes.

Figure 2.

Subcellular localization of ICS1 and ICS2. GFP fusion constructs were transiently expressed in tobacco cells by agroinfiltration. GFP signal (green) and chlorophyll autofluorescence (magenta) were observed using confocal microscopy. Magenta and green overlay is shown in white. Bars represent 10 µm.

Figure 3.

Functional complementation of the *PBB8 ICS*-deficient strain of *E. coli* by expression of Arabidopsis *ICS1* and *ICS2*. PBB8 cells were transformed with constructs expressing *ICS* and *ICS-GFP* fusions and spread onto CAS medium. Orange coloration indicate iron uptake from the medium and therefore restoration of siderophore production by a functional ICS activity. Bacteria were plated either on CAS medium without IPTG (A) or CAS medium containing 0.2 mM of IPTG (B).

Figure 4. Functional roles of *ICS1* and *ICS2*

A, phenotype of WT, *ics1*, *ics2* and *ics1 ics2* double mutant when grown *in vitro*. *ics1 ics2* double mutants can be more affected and display a more yellowish pigmentation. B and C, accumulation of isochorismate-derived compounds in the mutants: phylloquinone (B) and total SA accumulation following UV-induction (C).

Figure 5. Identification of SA in *ics1ics2* by GC-MS

SA in leaf extracts was silylated and separated by GC-MS. o-Anisic acid was used as internal standard. Panels A (wild type), B (*ics1ics2*) and C (SA standard) show the ion traces for m/z 209 (dotted line, characteristic for silylated o-anisic acid) and 267 (solid line, silylated SA). D, E, F depict the mass spectra for the peaks eluting at 10.8 min (arrows in panels A and B) for wild type, *ics1ics2* and the SA standard, respectively. The inset in panel F shows the fragmentation pattern of silylated SA.

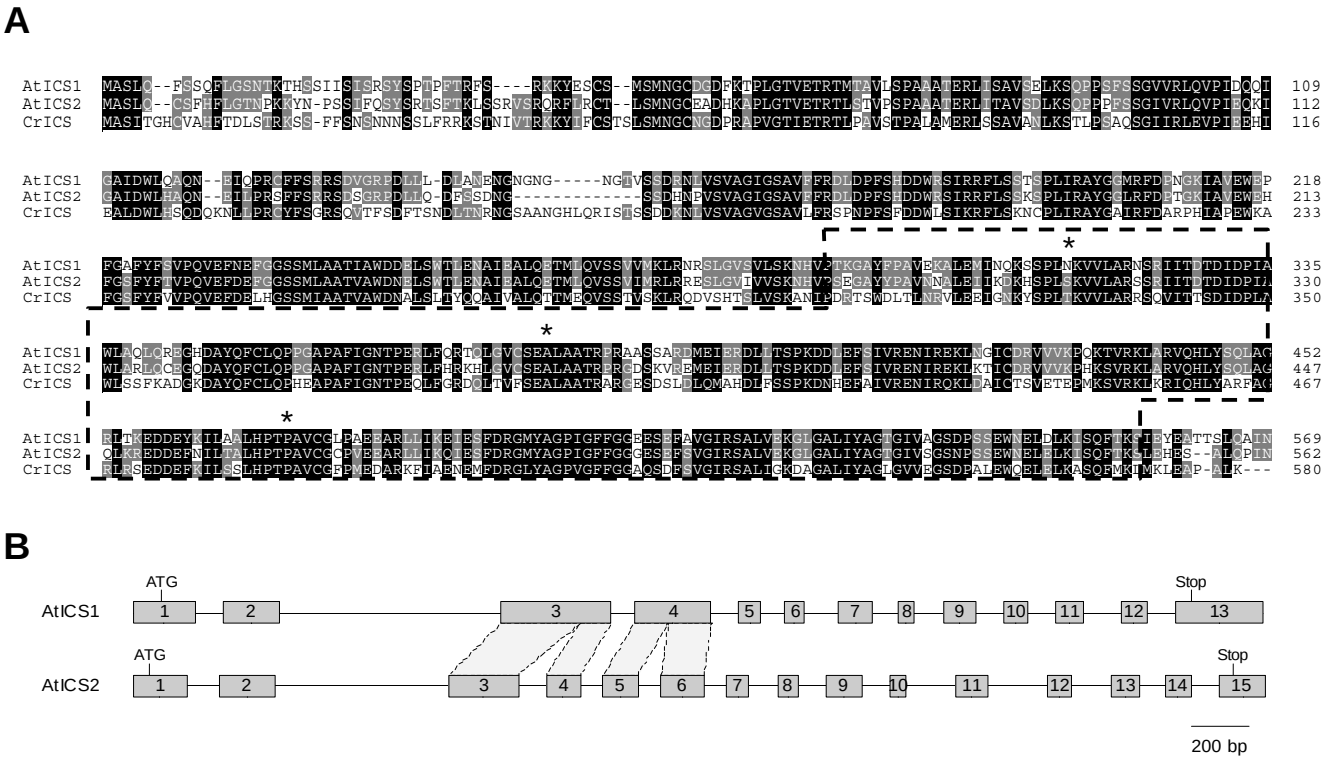

Figure 1. A. Sequence alignement of *Arabidopsis thaliana* ICS1(NP_565090) and ICS2 (ACC60228) and *Catharanthus roseus* ICS (CAA06837). The chorismate-binding domain is located in the dashed area and the position of residues conserved in ICS enzymes (Kolappan et al., 2007) is indicated with a star. B. exon/intron structure of *ICS1* and *ICS2*. Exons are represented by grey boxes and introns by thin lines. Sequence similarity between exon 3 of *AtICS1* and 3 and 4 of ICS2, and 4 of *AtICS1* and 5 and 6 of ICS2 is highlighted by dashes.

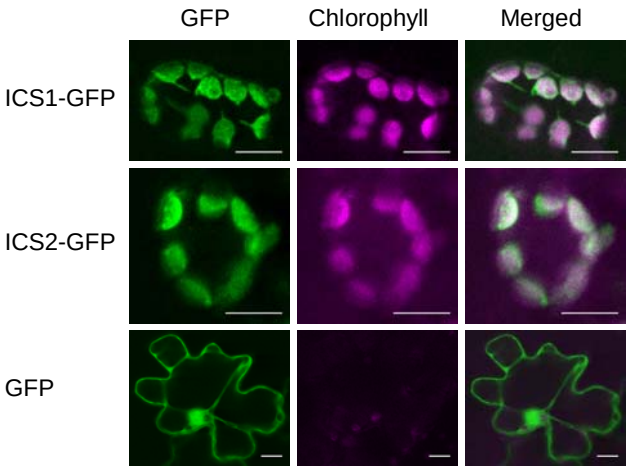

Figure 2. Subcellular localization of ICS1, ICS2 and control GFP. GFP fusion constructs were transiently expressed in tobacco cells by agroinfiltration. GFP signal (green) and chlorophyll autofluorescence (magenta) were observed using confocal microscopy. Red and green overlay is shown in white. Bars represent 10 µm.

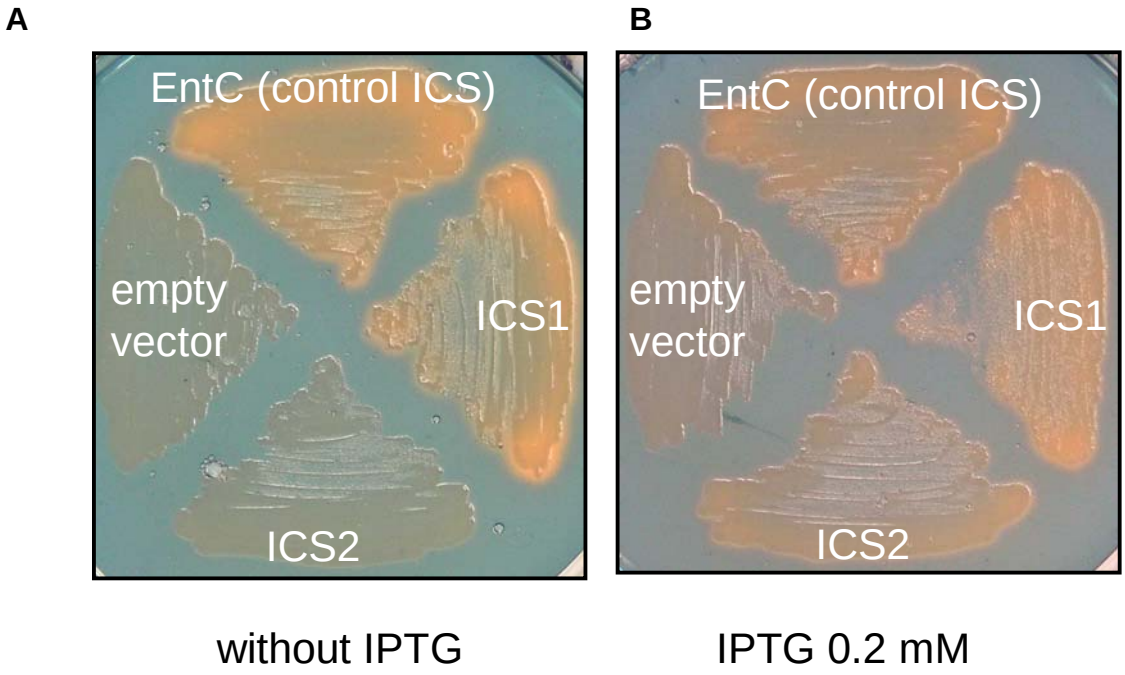

Figure 3. Functional complementation of the PBB8 ICS-deficient strain of *E. coli* by expression of Arabidopsis *ICS1* and *ICS2*. PBB8 cells were transformed with the various constructs and spread onto CAS medium. Orange coloration indicate iron uptake from the medium and therefore restauration of siderophore production, thus revealing a functional ICS activity. Bacteria were plated either on CAS medium without IPTG (A) or CAS medium containing 0.2 mM of IPTG (B).

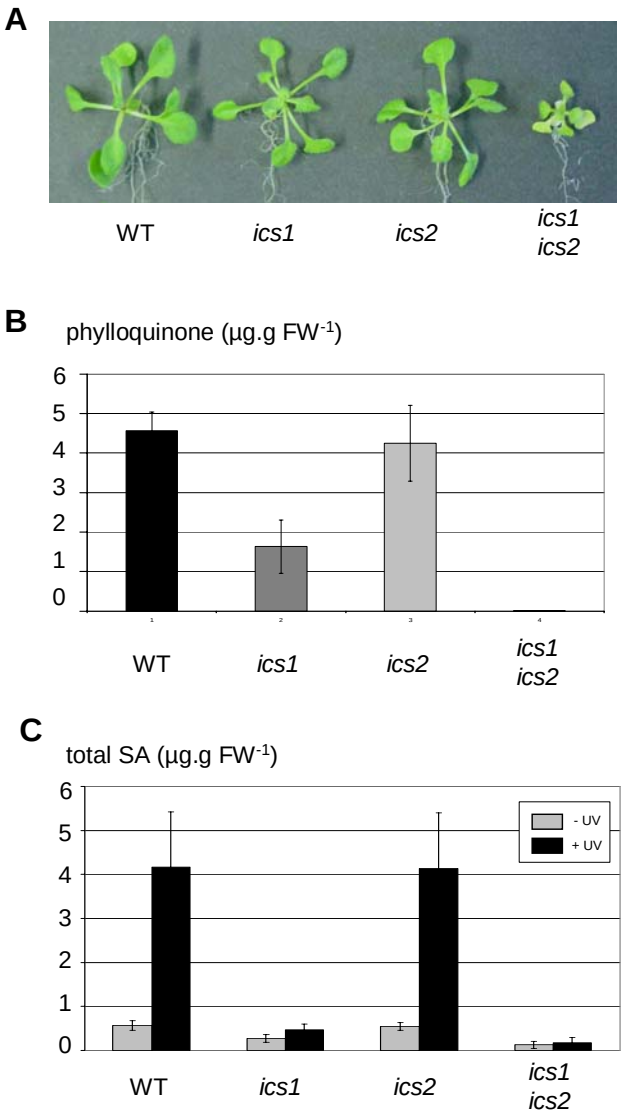

Figure 4. Functional roles of *ICS1* and *ICS2*
A. phenotype of WT, *ics1*, *ics2* and *ics1 ics2* double mutant when grown *in vitro*. B and C, accumulation of isochorismate-derived compounds in the mutants: phylloquinone (B) and salicylate accumulation following UV-induction (C).

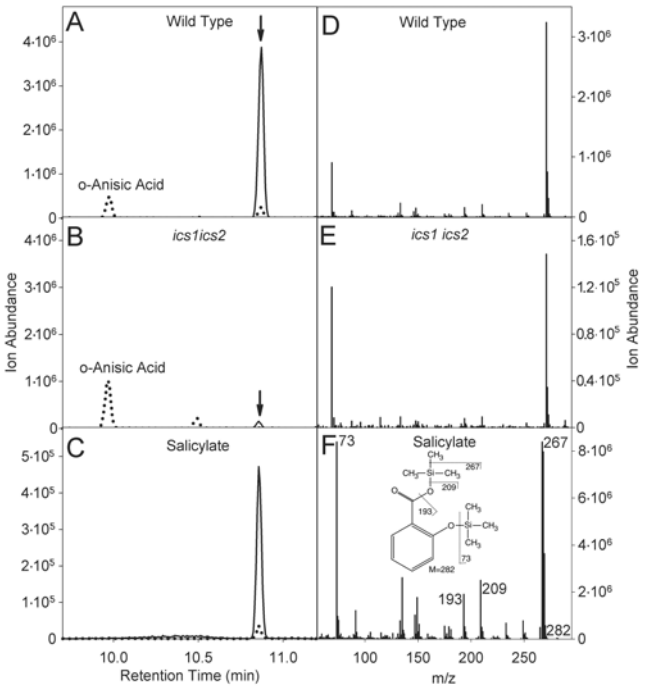

Figure 5. Identification of SA in *ics1ics2* by GC-MS.
SA in leaf extracts was silylated and separated by GC-MS. o-Anisic acid was used as internal standard. Panels **A** (wild type), **B** (*ics1ics2*) and **C** (SA standard) show the ion traces for m/z 209 (dotted line, characteristic for silylated o-anisic acid) and 267 (solid line, silylated SA). **D**, **E**, **F** depict the mass spectra for the peaks eluting at 10.8 min (arrows in panels **A** and **B**) for wild type, *ics1ics2* and the SA standard, respectively. The inset in panel **F** shows the fragmentation pattern of silylated SA.